



THE COLLEGE OF AERONAUTICS  
CRANFIELD

The Effect of Curvature on the Stress Concentrations\*  
Around Holes in Shells

- by -

D. S. Houghton\*\*, M.Sc.(Eng.), A.M.I.Mech.E., A.F.R.Ae.S.,

and

A. Rothwell, B.Sc., M.S., D.C.Ae.



SUMMARY

An experimental investigation has been carried out to investigate the effect of curvature on the stress concentrations around holes in shell structures. Two methods have been employed:-

- (1) Araldite cylinders, containing holes of various shapes, subjected to axial tension, internal pressure and torsion were examined by the photoelastic frozen stress technique.
- (2) Aluminium alloy curved panels and hemispheres were used in conjunction with miniature electrical strain gauges.

The results are compared with the theoretical solutions and suggest that the curvature effect can be significant, particularly for the case of shear or biaxial loading.

\* Paper presented to the Second International Conference on Stress Analysis, Paris, April 1962.

\*\* Associate Professor at The Royal Military College of Science, Shrivenham.

## CONTENTS

	<u>Page</u>
Summary	
Notation	
1. Introduction	1
2. Experimental Procedure	2
2.1. The Photoelastic Investigations	2
2.2. The Experiments on Curved Panels	4
2.3. The Experiments on the Hemi- spherical Shell	4
3. Theoretical Considerations	5
3.1. Flat Plate Theory	5
3.2. Circular Hole in Cylindrical Shell	6
3.3. Circular Hole in Spherical Shell	6
4. Discussion of Results	7
5. Conclusions	8
6. References	9
Figures	

## NOTATION

$f_1, f_2$	}	applied direct stresses
$f_x, f_y$		
$f_r, f_\theta$		radial and tangential direct stresses
$f'_r, f'_\theta$		radial and tangential bending stresses
$q$		applied shear stress
$\theta$		angle on circle or ellipse
$a$		radius of circular hole, or semi-major axis of elliptical hole
$b$		semi-minor axis of elliptical hole
$R$		radius of curvature of shell
$t$		sheet thickness
$\nu$		Poisson's ratio
$p$		internal pressure
$\alpha$		angle on the unit circle
$A, m$		constants in the transformation function

## 1. Introduction

In the analysis of the aircraft pressure cabin and the atomic reactor structure, a precise knowledge of the stress distribution around the various shaped openings is required. These may form windows or access doors, in which case their dimensions might be comparable with the overall dimensions of the shell, and clearly the determination of the stress concentrations around these openings is important.

It is generally considered that the factors which influence the magnitude of the stress concentration are the shape of the hole and the dimensions of the reinforcement, and provided that the hole size is small compared to the radius of the curvature of the shell, the geometry of the shell itself is thought to be of secondary importance.

In all the recent investigations the assumption has been made that shell curvature has little effect on the stress concentration around the hole, and to simplify the theoretical analysis the problem is considered to be identical to that of a hole in an infinite plane sheet.

Little experimental work has been published to justify this assumption; in fact most of the experimental work which is available<sup>(1, 2)</sup> has been carried out on flat plates, owing to the simplification of the necessary apparatus.

One previous attempt to study the stresses around circular and elliptical holes in cylinders was carried out by Richards<sup>(3)</sup> on Xylonite models. The stresses were measured by standard electrical strain gauge techniques in conjunction with an automatic strain gauge recorder. The results indicated that significant bending stresses arise in the vicinity of the hole, and Richards concluded that the 'flat plate' theory is inadequate to completely describe the stress distributions around the hole.

A closer examination of these papers suggests that for an unreinforced hole in a shell subjected to internal pressure this discrepancy is not unreasonable, since much depends upon whether the transverse pressure loading across the hole is allowed to be reacted at the edge of the hole, or whether this is reacted externally. The flat plate theory when applied to unreinforced holes does not make allowance for the effect of out of plane forces. For the reinforced hole, it is generally considered that provided the hole is neutral, or nearly so, and the transverse loading is applied in a prescribed manner<sup>(1)</sup>, then close agreement should be obtained with the flat plate solution. In other words, the stress concentrations arising in the vicinity of an unreinforced hole in a curved shell will be in excess of those given by flat plate theory, but if the hole is suitably reinforced it is considered that the discrepancies should become insignificant.

The theoretical analysis of the stress distribution around holes in circular cylinders is restricted to very small unreinforced circular holes. The solution for the biaxial loading case is given by Lurie<sup>(5)</sup>, and this solution has been discussed by Penney<sup>(7)</sup>. Lurie's solution has been extended by Withum<sup>(6)</sup> to the case of a cylinder subjected to torsion, and again the solution is restricted to very small holes. The solution for a circular hole in a spherical shell under internal pressure may be derived from the general solution given by Novozhilov<sup>(9)</sup>,

subject to certain conditions on the size of the hole. An alternative solution is given by Penney<sup>(8)</sup>.

The results of a number of experiments which were undertaken<sup>(4)</sup> to investigate the significance of the effect of curvature on the stress concentration around circular and elliptical holes are reported. A series of photoelastic experiments using the frozen stress method has been conducted on unreinforced circular and elliptical holes in Araldite cylinders, subjected to various loading conditions. A further series of tests was carried out to find the effect of curvature on the stress concentrations around unreinforced circular holes in curved panels and in a hemispherical shell, using electrical strain gauges.

The hole dimensions are comparable with the large openings which occur in many pressure vessel designs, and in consequence are in excess of those given by the limits of the Lurie-Withum solution for cylindrical shells.

The experimental results are compared with the various theoretical solutions and also with the corresponding flat plate solution.

## 2. Experimental Procedure

In order to study the effect of shell curvature on the stress concentrations around unreinforced holes, the following series of experiments were conducted:

- (a) Photoelastic investigations using Araldite cylinders which contained either circular or elliptical holes.
- (b) Experiments on curved aluminium alloy panels containing a circular hole.
- (c) Experiments on a hemispherical shell having a circular hole.

### 2.1. The Photoelastic Investigations

#### The Range of the Experiments

The cylinders under test were cast from Araldite B and Hardener 901, as supplied by Aero Research Ltd., in the ratio of four to one, and machined to the dimensions given in Fig. 1. Three sizes of circular hole having diameters 0.8 in., 1.0 in. and 1.2 in., were examined. In addition an elliptical hole having a minor axis 0.85 in. and major axis 1.2 in. (with its minor axis parallel to the longitudinal axis of the cylinder) was later examined. The apparatus shown in Fig. 2 enabled the cylinders to be loaded by axial tension, torsion or internal pressure.

The frozen stress technique was used to study the stress concentrations in the vicinity of the holes. This method was found convenient since only small externally applied forces were required. Also, in the case of internal pressure loading, the presence of the sealing plug covering the hole made it necessary to remove the loading before analysing the stresses.

The arrangement of the polariscope to measure the mean stresses in the cylinder is shown in Fig. 3. A simple crossed diffuse light polariscope was used

with monochromatic sodium light. The polariser was set inside the cylinder, with the hole under examination between it and the analyser. By this arrangement, stresses in the far wall of the cylinder did not interfere with those being measured.

#### The Specimen Loading Mechanism

Since the specimen was loaded at temperature the available oven size dictated the overall dimension of the loading mechanism. The oven was a Towers thermostatically controlled electric oven, and the loading rig consisted essentially of two parts:

- (a) A frame for holding the specimen, together with the necessary mechanism for applying tension and torsion.
- (b) The pressurisation equipment.

The tensile load was applied by weights applied at the end of a 4:1 lever arm attached by a flexible cable to the centre of the top plate of the cylinder. Torsion was applied by weights attached by cables around a 5.4 in. dia. disc which was screwed to the top plug. Arrangements were made to counterbalance the weight of this disc during the experiment.

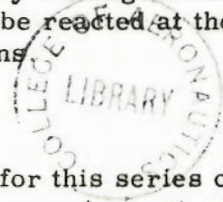
The pressurisation equipment was designed to give a constant pressure, and to compensate for variations in the air volume in the system due to temperature changes. This was achieved by using a balloon as an air reservoir to which pressure was applied by a constant head of water. The pressure was measured on a water manometer and could be varied by altering the height of the constant head. It was found that this method could control the internal pressure of 1 lb/in<sup>2</sup> to within 0.5 per cent during the time the specimen was cooling from 130°C.

During pressurisation of the cylinder, the holes were sealed by a metal plug which was covered inside the cylinder by thin polythene sheeting held in position by a thin film of silicone oil. The polythene had the advantage of softening at temperature and taking up the contour of the cylinder wall. Initially this plug was supported externally (method 'A') so that the pressure loading on the hole would not be carried by the cylinder. This method was intended to minimise bending stresses at the edge of the hole. The tests were subsequently repeated using a very thin, flexible metal plug which was supported by the edge of the hole (method 'B') so that the pressure loading on the hole would be reacted at the edge. This method is more consistent with the theoretical solutions.

#### The Frozen Stress Technique

The frozen stress method was found to be satisfactory for this series of experiments. The identification of the fringes proved quite easy in most cases. Because of the limited space inside the cylinders, the Senarmont method of determining the fractional fringe order was employed since it did not require a quarter wave plate between the polariser and the specimen.

The main disadvantage of the frozen stress method was the presence of compressive edge effects which appeared with time, but this could be overcome



by analysing the cylinder as soon as possible after the specimen had been removed from the oven. By examining the cylinder without slicing, the mean value of the stress was obtained. The method of testing does not allow bending stresses in the cylinder to be measured.

## 2.2. The Experiments on Curved Panels

A series of experiments were conducted using four L.72 aluminium alloy curved panels (Fig. 4) which were 20 in. long and 10 in. developed width, containing a 2 in. diameter circular hole. The panel dimensions were chosen to give an adequate variation of parameter  $\frac{a^2}{Rt}$ .

The dimensions of the panels used in this series of experiments were:

Panel No.	Radius of Curvature (in.)	Thickness (in.)
1	6	.028
2	6	.022
3	12	.022
4	12	.036

The panels were loaded in tension in a standard tensile testing machine. A number of special end plates were designed to minimise bending effects in the panel. A preliminary series of experiments indicated that the panel dimensions were such that panel end effects did not disturb the stress distribution in the vicinity of the hole.

Strains were measured by means of Tinsley 6H electrical resistance strain gauges with a conventional strain gauge recorder. The strain gauge positions are shown in Fig. 5.

## 2.3. The Experiments on the Hemispherical Shell

Only one specimen was tested for this series of experiments. This consisted of a 16 in. diameter hemispherical shell containing a 3 in. diameter hole, made by spinning a sheet of 16 s.w.g. (0.064 in.) L.59 aluminium alloy sheet (Fig. 6). This method of manufacture has proved satisfactory for making hemispheres, although some variation in thickness around the contour of the hemisphere was to be expected. It was found that in the region of the hole the thickness was substantially constant at 0.062 in.

A wooden plug with a standard 1/8 in. diameter 'O' ring was used to seal the specimen (Fig. 7) which was pressurised using air at 18 lb/in<sup>2</sup>. The stresses were measured by Tinsley 6H and 6K electrical strain gauges located as shown in Fig. 8, together with a Savage and Parsons strain gauge recorder.

### 3. Theoretical Considerations

#### 3.1. Flat Plate Theory (Fig. 16)

The solution for the stresses around an unreinforced elliptical hole in an infinite plane sheet may be obtained by the use of the complex stress function and the method of conformal transformation<sup>(1)</sup>.

The transformation function

$$z = A \left( \zeta + \frac{m}{\zeta} \right)$$

transforms an ellipse in the  $z$ -plane on to the unit circle in the  $\zeta$ -plane, where

$$m = \frac{a - b}{a + b} ,$$

and  $a, b$  are the semi-major and semi-minor axes respectively. Complex stress functions are found which satisfy the boundary conditions at the edge of the hole and at infinity.

For an elliptical hole in a plate subjected to uniform biaxial tensions  $f_x$  and  $f_y$ , the stress  $f_\theta$  at the edge of the hole is given by

$$f_\theta = \frac{(f_x + f_y)(1 - m^2) + 2(f_x - f_y)(m - \cos 2\alpha)}{1 + m^2 - 2m \cos 2\alpha} ,$$

and when the plate is subjected to uniform shear  $q$  the edge stress is

$$f_\theta = \frac{4q \sin 2\alpha}{1 + m^2 - 2m \cos 2\alpha} .$$

The angle  $\alpha$  is the angle on the unit circle, and the corresponding angle  $\theta$  on the ellipse is given by

$$\tan \theta = \frac{b}{a} \tan \alpha .$$

For a circular hole

$$m = 0 ,$$

and the expression for the edge stress under biaxial tension reduces to

$$f_\theta = (f_x + f_y) - 2(f_x - f_y) \cos 2\theta ,$$

and under uniform shear

$$f_\theta = 4q \sin 2\theta ,$$

where  $\theta$  is the true angle on the circle.



### 3.2. Circular Hole in Cylindrical Shell (Fig. 17)

The solution for a small circular hole in a cylindrical shell under uniform biaxial tension has been given by Lurie<sup>(5)</sup>. The solution is restricted to very small holes for which

$$\frac{a^2}{Rt} \ll 1 ,$$

where  $a$  is the radius of the hole,

$R$  is the radius of curvature of the cylindrical shell

and  $t$  is the sheet thickness.

When the shell is subjected to biaxial tensions  $f_x$  and  $f_y$ , the direct stress  $f_\theta$  at the edge of the hole is given by

$$f_\theta = (f_x + f_y) - 2(f_x - f_y) \cos 2\theta + \sqrt{3(1 - \nu^2)} \cdot \frac{\pi}{4} \cdot \frac{a^2}{Rt} \left[ 2 f_y - (f_x - 3 f_y) \cos 2\theta \right] .$$

Lurie also obtains expressions for the bending stress in the shell at the edge of the hole.

The corresponding solution for the case of uniform shear is given by Withum<sup>(6)</sup>, with the same restriction on hole size. In this case the stress at the edge of the hole is given by

$$f_\theta = q \left[ 4 + \sqrt{3(1 - \nu^2)} \cdot \frac{\pi}{2} \cdot \frac{a^2}{Rt} \right] \sin 2\theta .$$

### 3.3. Circular Hole in Spherical Shell

A solution for the stress concentration around a circular hole in a spherical shell may be obtained from the general equations for spherical shells given by Novozhilov<sup>(9)</sup>. The solution is not applicable to very small values of the curvature parameter ( $a^2/Rt \ll 1$ , approximately) where  $R$  is the spherical radius.

The direct stress  $f_\theta$  at the edge of the hole in a spherical shell subjected to internal pressure  $p$  is given by

$$f_\theta = \frac{pR}{2t} \left[ 1 + \sqrt[4]{48(1 - \nu^2)} \cdot \sqrt{\frac{a^2}{Rt}} \right] ,$$

if the ratio  $a/R$  is small ( $a/R \ll \frac{1}{3}$ , approximately) and there are no bending stresses at the edge of the hole according to this solution.

An alternative solution has been given by Penney<sup>(8)</sup>, for which expressions for the edge stress may be written approximately:

In the range  $0 < \sqrt{\frac{a^2}{Rt}} < 0.5$

$$f_{\theta} = \frac{pR}{2t} \left[ 2 + 2.6 \frac{a^2}{Rt} \right],$$

and for

$$\sqrt{\frac{a^2}{Rt}} > 0.5$$

$$f_{\theta} = \frac{pR}{2t} \left[ 1.2 + 2.58 \sqrt{\frac{a^2}{Rt}} \right].$$

(Taking  $\nu = \frac{1}{3}$ ) and in this case the bending stresses at the edge of the hole are not zero.

#### NOTE

In the theoretical solutions for a sealed hole in a cylindrical or spherical shell under internal pressure, it is assumed that the pressure loading on the hole is reacted by a shear force at the edge of the hole, so that this part of the loading is carried by the shell itself.

#### 4. Discussion of Results

The results of the photoelastic investigations on circular and elliptical holes in the Araldite cylinders, under various loading conditions, are shown in Figs. 9, 10 and 11.

For the torsion loading case it is found that shell curvature has a significant effect on the stress concentration around the hole. For the circular hole the maximum stress concentration increases with hole diameter, and for the largest hole tested (1.2 in. dia.) the maximum stress concentration exceeds the flat plate theory by about 40 per cent. It is also found that the position of maximum stress changes with increase in hole diameter. Although only one size of elliptical hole was tested, it would appear that the effects of curvature are similar.

When the cylinder is subjected to internal pressure, little increase in the stress concentration due to curvature is obtained if the pressure loading on the hole is reacted externally. This is probably due to an effective reduction in the local pressure loading in the vicinity of the hole. However, if the pressure on the hole is reacted at the edge of the hole so that this part of the loading is supported by the shell itself, a significant increase in the stress concentration is obtained.

When the cylinder is subjected to axial tension no increase in stress concentration is found.

In Fig. 11, the variation of the maximum stress concentration with the curvature parameter  $\sqrt{a^2/Rt}$  is plotted for the circular holes, and a comparison is made with the theoretical solutions of Lurie and Withum, which are restricted to values of the curvature parameter  $a^2/Rt \ll 1$ .

In practical applications the value of the curvature parameter  $a^2/Rt$  may greatly exceed unity, and to investigate the effect of curvature for larger values

of this parameter a further series of tests was carried out on a number of curved panels, containing a circular hole, subjected to axial tension. These results are shown in Fig. 12. It is found that for the larger values of  $a^2/Rt$ , the curvature effect becomes significant, and flat plate theory is inadequate to predict the maximum stress concentrations.

In order to show the effect of curvature on the stress concentrations around holes in spherical shells under internal pressure, a test was carried out on a hemispherical shell containing a circular hole. Fig. 13 shows the variation of the theoretical maximum stress concentration (obtained from Ref. 8) with the parameter  $a^2/Rt$ . For one particular diameter of hole ( $\sqrt{a^2/Rt} = 2.09$ ) the experimental results of the variation of the radial and tangential direct stresses with the distance from the edge of the hole are given in Fig. 14, and the corresponding results for the radial and tangential bending stresses in the shell are given in Fig. 15. These results are compared with the theoretical solution derived from Ref. 9. Good general agreement is obtained, although the theoretical results are somewhat in excess of the experimental. The maximum stress concentration is found to be considerably greater than that predicted by flat plate theory, and it is seen that the bending stresses away from the edge of the hole are significant.

#### 5. Conclusions

The effect of curvature on the stress concentrations around holes in shells may be considerable in many cases, particularly for holes in a cylinder under torsion or internal pressure, and for holes in a spherical shell under internal pressure.

For internal pressure loading, the stress concentration also depends on the method of supporting the pressure on the sealed hole.



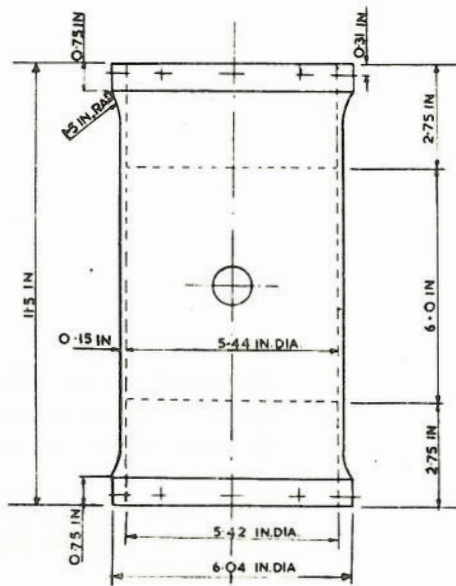


FIG. 1. DIMENSIONS OF ARLDITE CYLINDERS

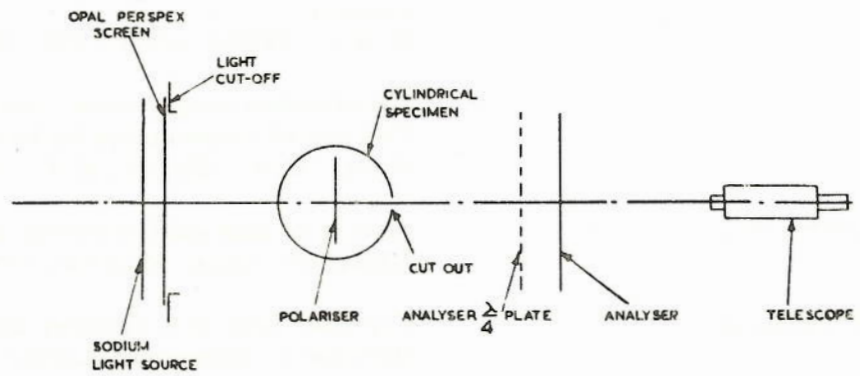


FIG. 3. ARRANGEMENT OF POLARISCOPE

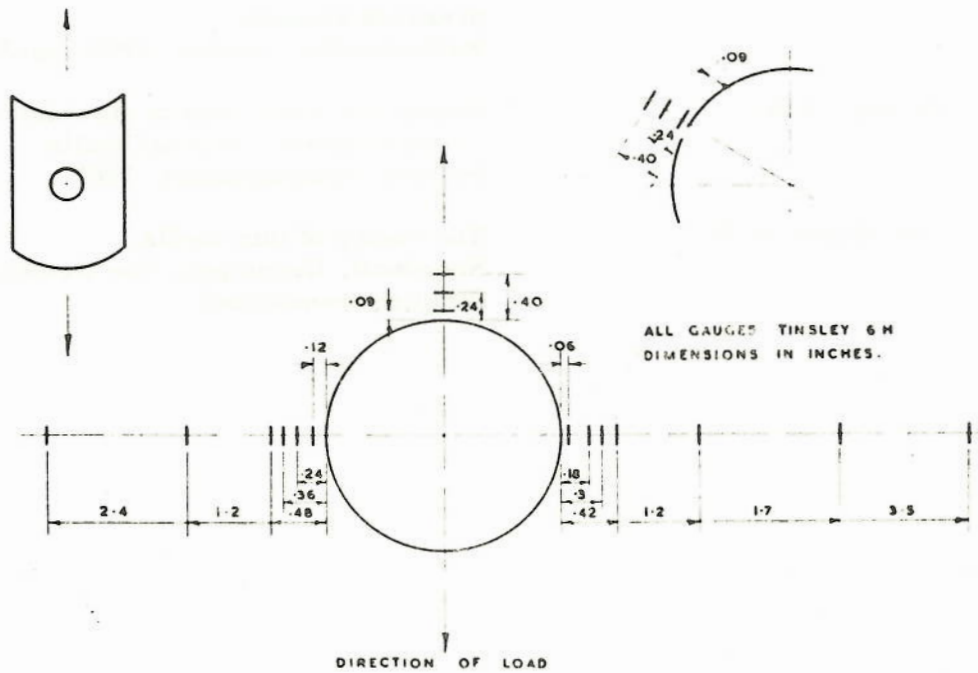


FIG. 5. STRAIN GAUGE POSITIONS FOR TESTS ON CURVED PANELS

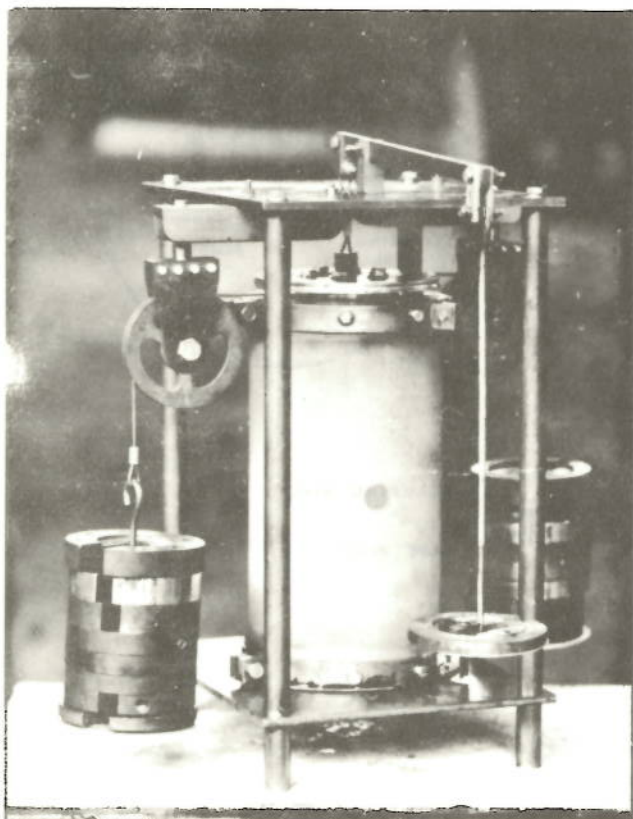


FIG. 2. LOADING RIG FOR PHOTO-ELASTIC TESTS ON ARALDITE CYLINDERS

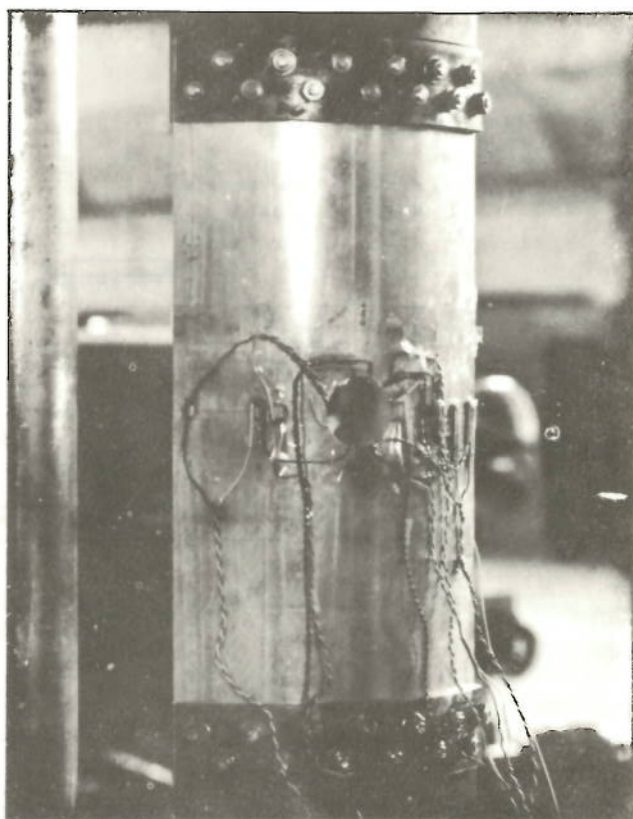


FIG. 4. CURVED PANEL CONTAINING A CIRCULAR HOLE

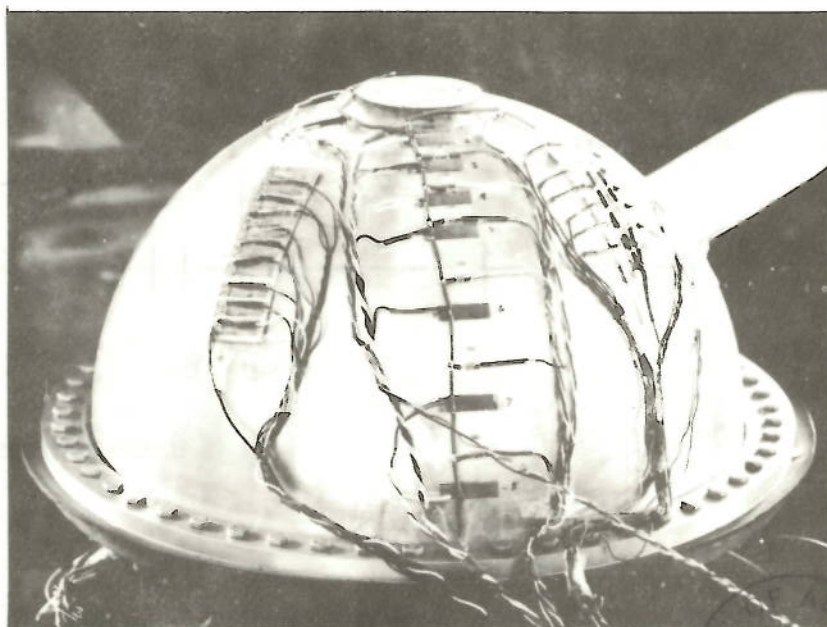


FIG. 6. HEMISPHERICAL SHELL CONTAINING A CIRCULAR HOLE

COLLECTED LIBRARY FROM PAUTICS

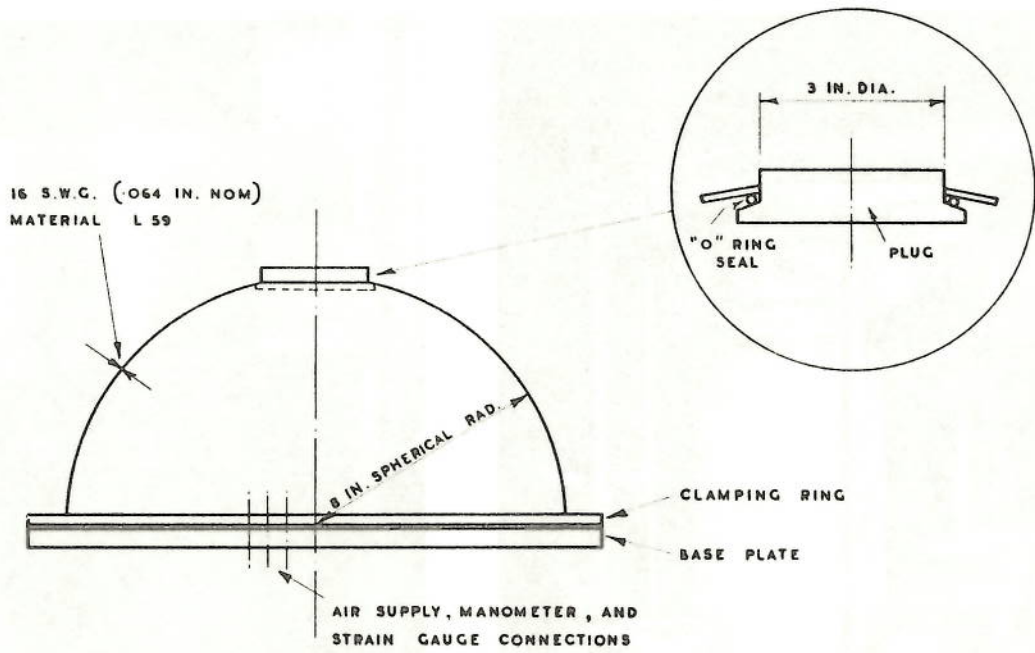


FIG. 7. DIMENSIONS AND METHOD OF SEALING OF HEMISPHERICAL SHELL

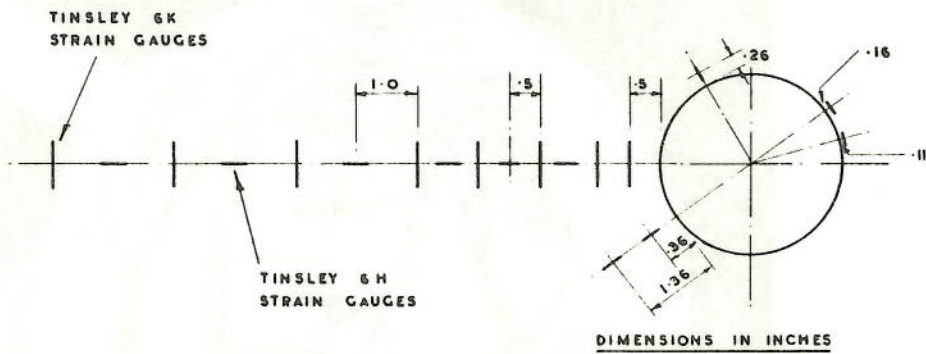
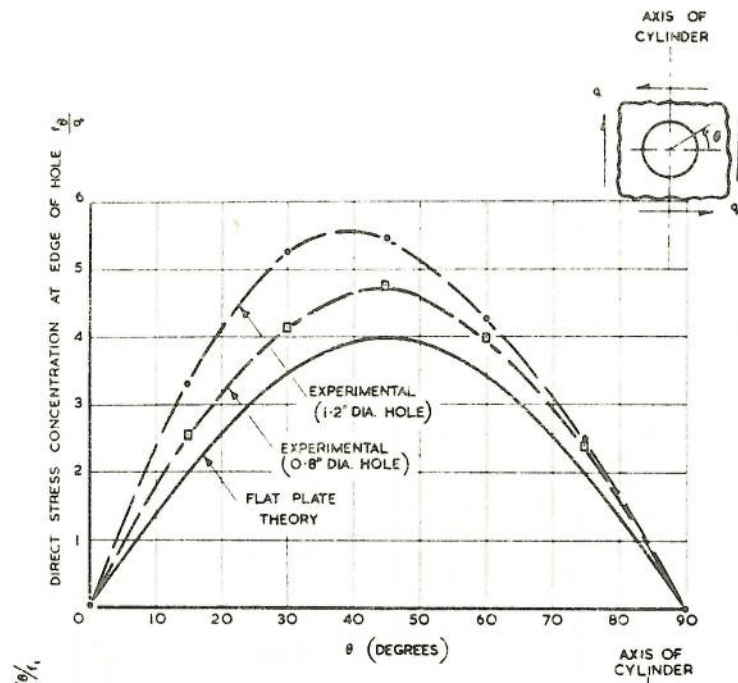
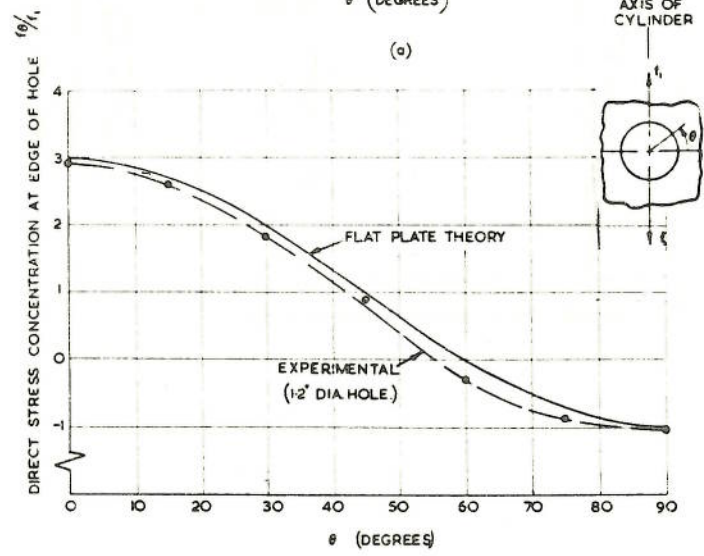


FIG. 8. STRAIN GAUGE POSITIONS FOR TESTS ON HEMISPHERICAL SHELL

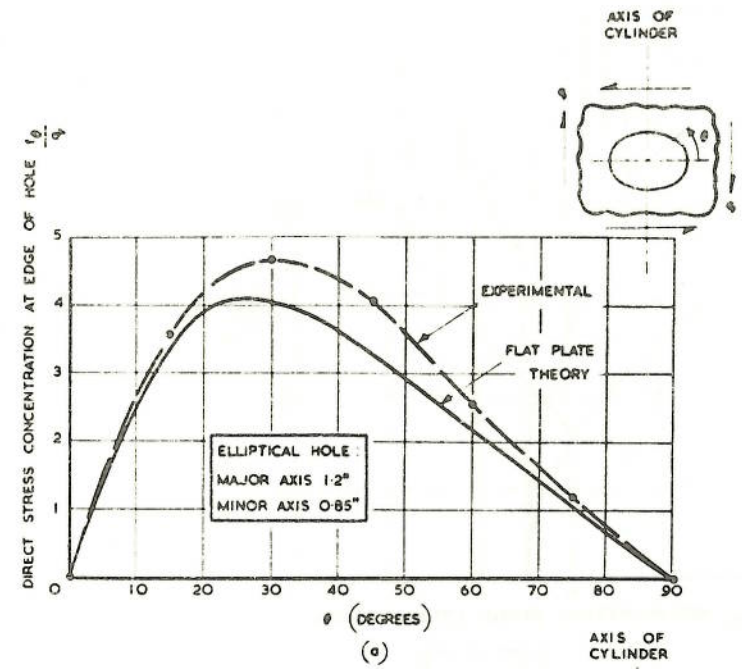


(a)

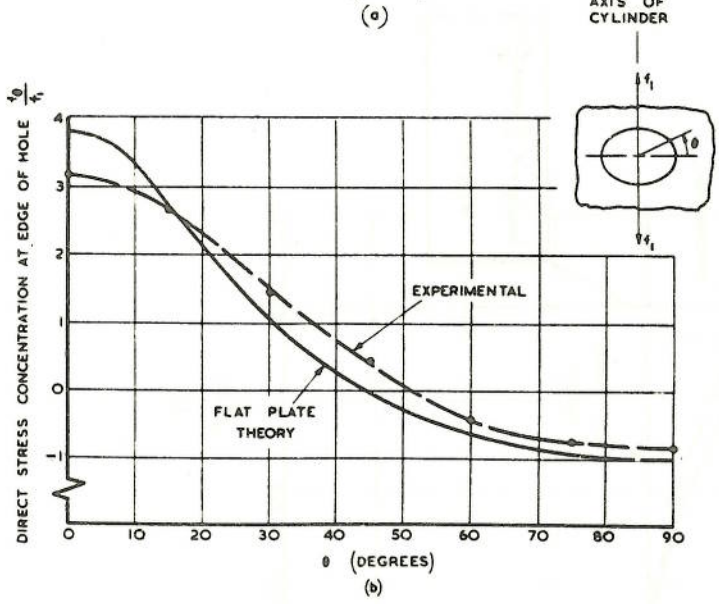


(b)

FIG. 9. PHOTOELASTIC TESTS ON CIRCULAR HOLE IN CYLINDER: STRESS DISTRIBUTION UNDER TORSION AND AXIAL TENSION



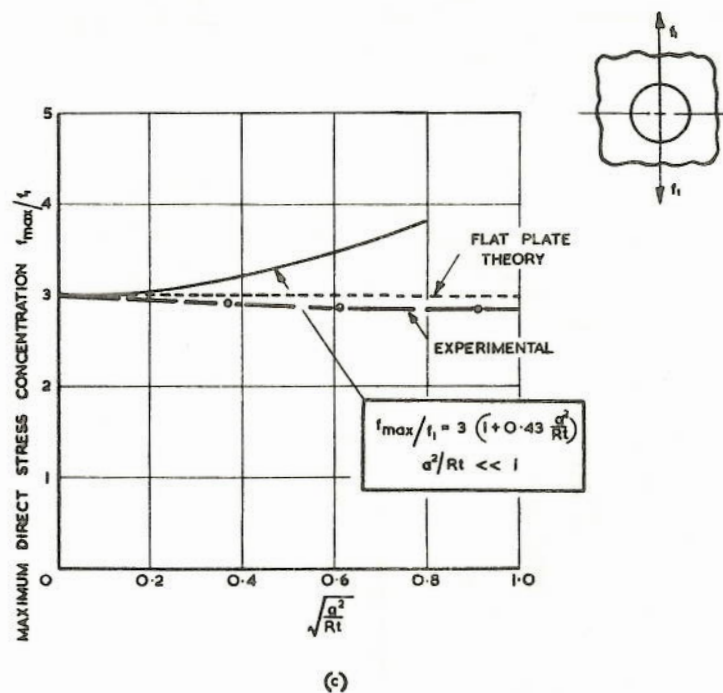
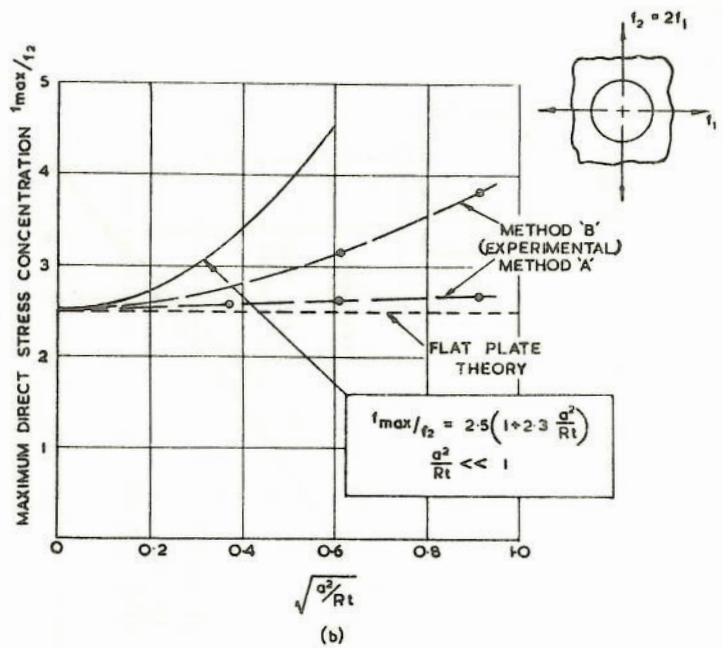
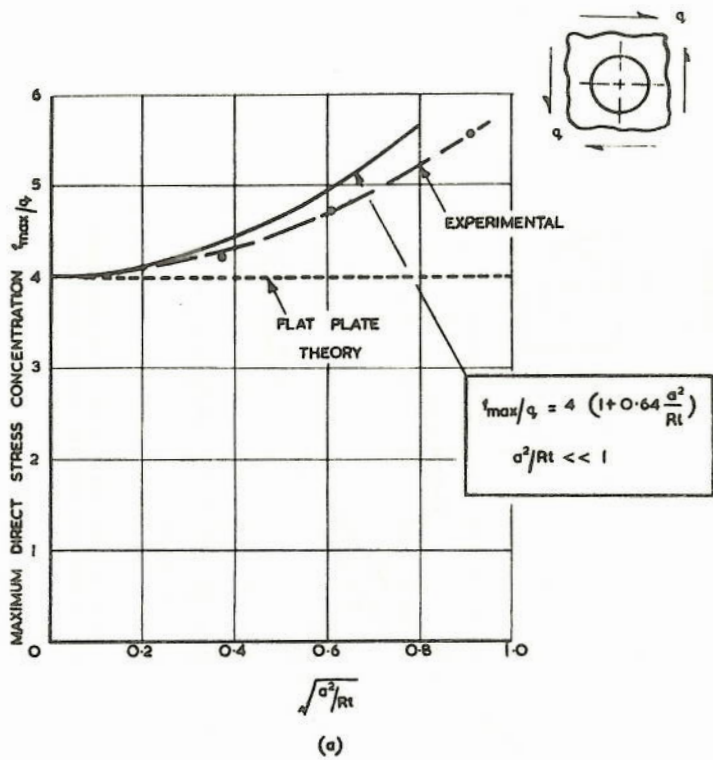
(a)



(b)

FIG. 10. PHOTOELASTIC TESTS ON ELLIPTICAL HOLE IN CYLINDER: STRESS DISTRIBUTION UNDER TORSION AND AXIAL TENSION





RADIUS OF HOLE	$a$
RADIUS OF CYLINDER	$R$
SHEET THICKNESS	$t$

FIG. 11 PHOTOELASTIC TESTS: MAXIMUM STRESS CONCENTRATION FOR CIRCULAR HOLE IN CYLINDER UNDER TORSION, INTERNAL PRESSURE AND AXIAL TENSION

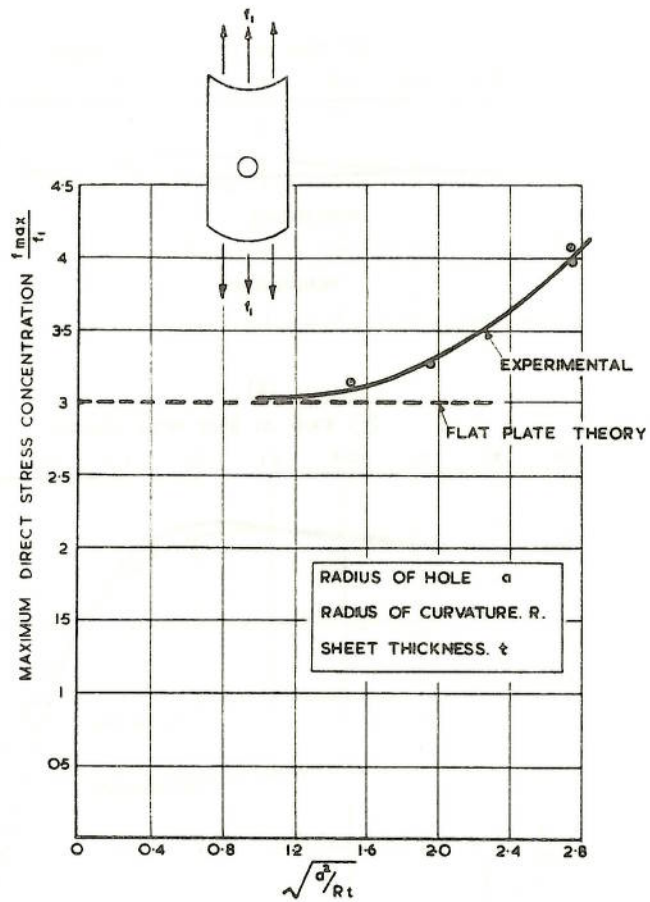


FIG.12. TESTS ON CIRCULAR HOLE IN CURVED PANEL UNDER AXIAL TENSION: MAXIMUM STRESS CONCENTRATION

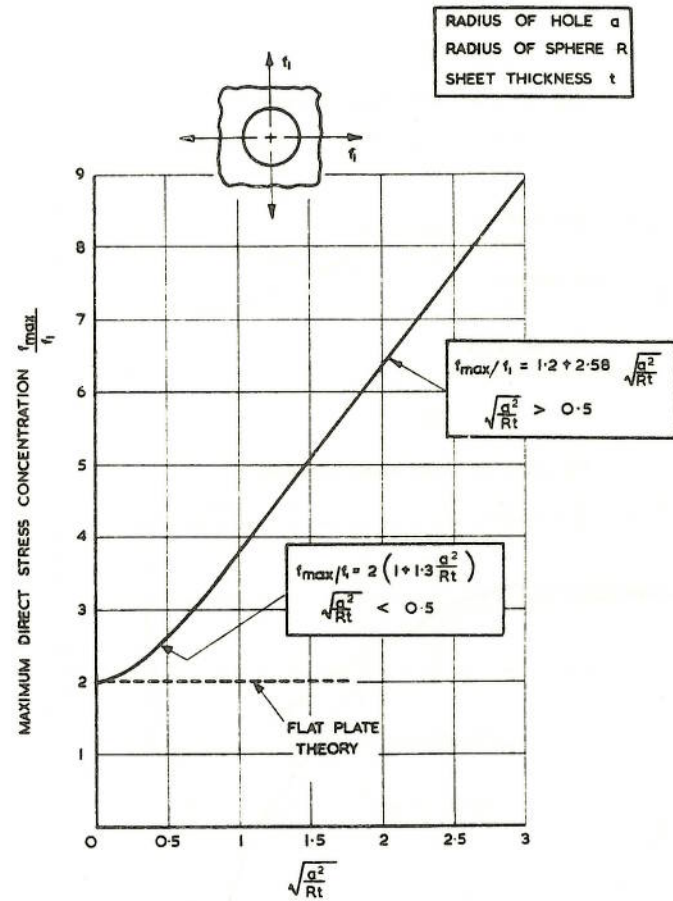
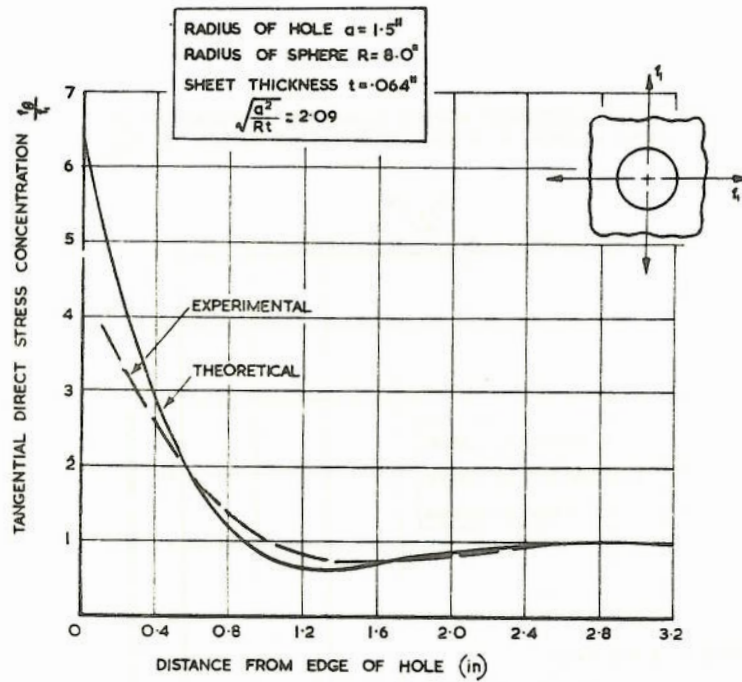
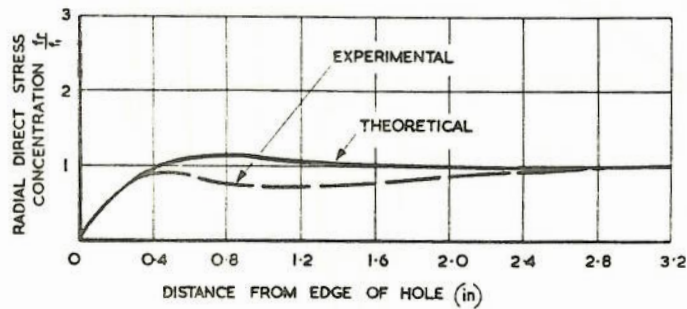


FIG.13. THEORETICAL MAXIMUM STRESS CONCENTRATION FOR CIRCULAR HOLE IN SPHERICAL SHELL UNDER INTERNAL PRESSURE

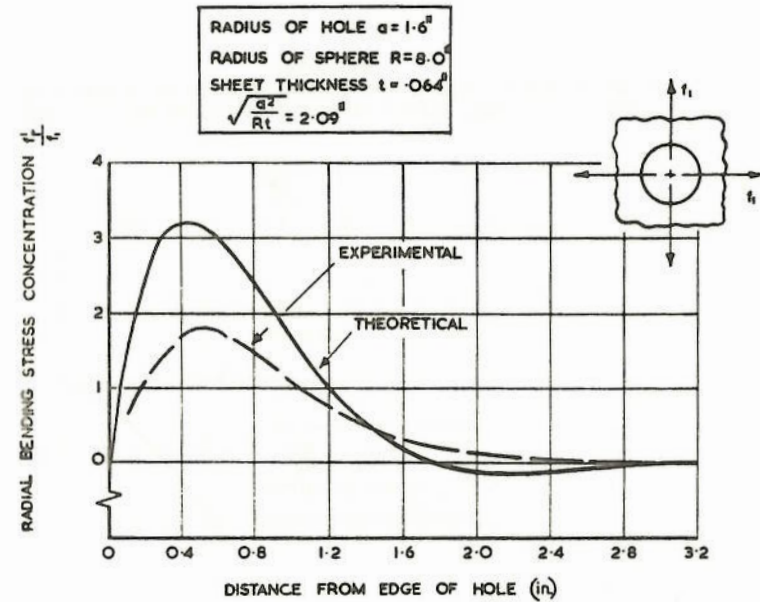


(a)

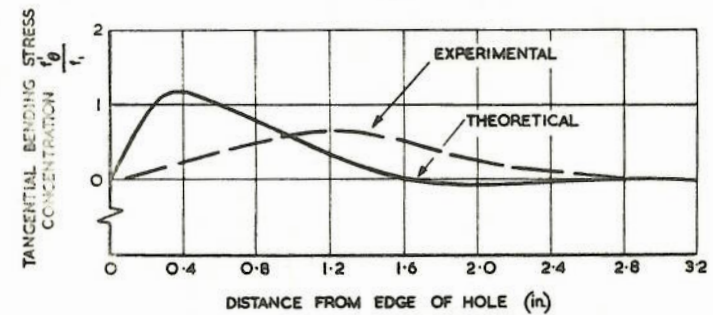


(b)

FIG. 14. TESTS ON CIRCULAR HOLE IN HEMISPHERICAL SHELL UNDER INTERNAL PRESSURE: RADIAL AND TANGENTIAL DIRECT STRESS DISTRIBUTIONS



(a)



(b)

FIG. 15. TESTS ON CIRCULAR HOLE IN HEMISPHERICAL SHELL UNDER INTERNAL PRESSURE: RADIAL AND TANGENTIAL BENDING STRESS DISTRIBUTIONS

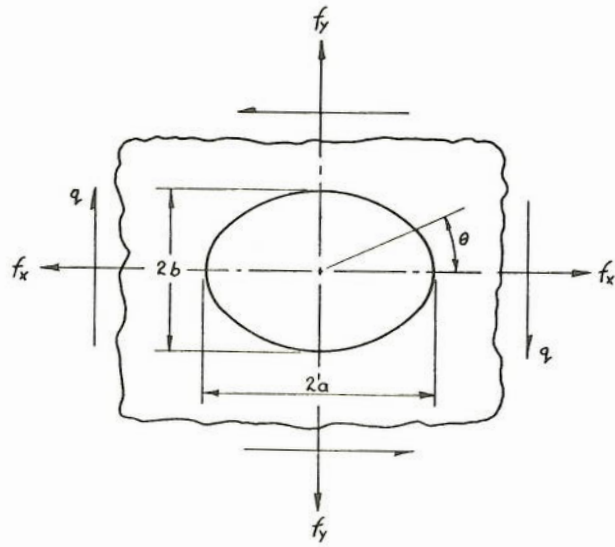


FIG. 16. NOTATION FOR ELLIPTICAL HOLE IN A PLANE SHEET

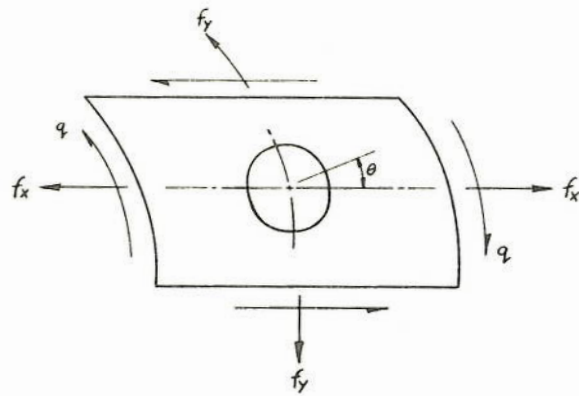


FIG. 17. NOTATION FOR CIRCULAR HOLE IN CYLINDER